RSC Advances

ROYAL SOCIETY OF CHEMISTRY

www.rsc.org/advances

Specific depletion of protein using polydopamine imprinting shells modified amino-functionalized magnetic nanoparticles

Ruixia Gao,[*a] Lili Zhang,[b] Yi Hao,[b] Xihui Cui,[b] Yuhai Tang[*a,b]

[a] Institute of Analytical Science, School of Science, Xi'an Jiaotong University, Xi'an 710049, P. R. China. E-mail: ruixiagao@mail.xjtu.edu.cn; tyh57@mail.xjtu.edu.cn. Tel./Fax: +86 029 8265 5399.

[b] College of Pharmacy, Xi'an Jiaotong University, Xi'an 710061, P. R. China.

Abstract

Thin imprinting shell over functionalized magnetic nanoparticles is an effective solution to weaken mass transfer resistance, achieve high binding capacity, and attain rapid separation. In this work, a simple, green, and resultful approach was developed to imprint bovine serum albumin (BSA) on the surface of amino-modified Fe_3O_4 nanoparticles (Fe_3O_4@NH_2) using dopamine as monomer through a two-step immobilized template strategy. The results of X-ray diffraction and vibrating sample magnetometer indicated that the as-synthesized nanomaterials exhibited high crystallinity and satisfactory superparamagnetic properties. Transmission electronic microscopy and Fourier transform infrared spectroscopy of the products showed that polydopamine shells successfully attached onto Fe_3O_4@NH_2. The polydopamine shells with a thickness of about 10 nm enables the template recognition sites to be accessed easily, and exhibits fast kinetics and high adsorption capacity in aqueous solution. Meanwhile, a excellent selectivity towards BSA had been presented when employed bovine hemoglobin (BHb), transferrin, and immunoglobulin G (Ig G) as competitive proteins. Good recovery after a reasonably mild elution and successful capture of the target protein from a real sample of bovine blood suggested its potential value in practical applications. In addition, the resultant polymers were stable and had no obvious deterioration after at least six adsorption-regeneration cycles. The versatility of the proposed method had also been verified by choosing four other proteins with different isoelectric points as the templates.

Keywords: Surface imprinting; Magnetic separation; Protein recognition; Polydopamine; Immobilized template strategy

1. Introduction

Affinity separation and removal of high-abundant proteins from blood plasma is often used as a sample pretreatment technique before clinical and pharmaceutical proteomic studies. Several feasible methods, such as immobilized metal affinity chromatography (IMAC),[1,2] dielectrophoresis,[3,4] and immunoaffinity chromatography[5,6] have been applied to remove high-abundant proteins in biological samples. However, there are some drawbacks, including valuableness, time and labor consuming, poor stability, limitations of the targets, and non-reusability that prohibit the widespread applicability of these approaches. Therefore, to develop a more effective and general application method for specific isolation and depletion of high-abundant proteins is of vital significance.

Molecularly imprinted polymers (MIPs), tailor-made receptors with specific three-dimensional recognition sites complementary in shape, size, and functionality with the templates,[7,8] are considered as one of the most promising affinity matrix. MIPs have also been regarded as a satisfactory adsorbent for separation and removal of target protein,[9,10] as a result of good physical, chemical, and thermal stability, simple and economical production, durability, reusability, as well as high specificity. With respect to protein imprinting, a big problem is the large molecular size which restricts the mass transfer of proteins between the cross-linked polymer network and solution. Another problem is aqueous media where proteins prefer to exist, but the noncovalent interactions of templates and monomers can be reduced remarkably. Other problems contain flexible conformation, complexity, and numbers of functional groups, all of which are unfavorable elements for imprinting protein.

Some imprinting approaches have been developed to solve the mass transfer difficulty of protein, for example, surface imprinting,[11,12] epitope imprinting,[13,14] and metal-coordination polymerization.[15,16] Among these, surface imprinting with the recognition cavities located at the surface of MIPs, expecting to weaken mass transfer resistance and make the removal of the template protein easy and complete, is regarded as the most promising method for imprinting protein.[17,18] Nanomaterials are

ideal supporters for surface imprinting especially magnetic Fe_3O_4 nanoparticles (NPs), due to their superparamagnetism and simple preparation.[19,20] These excellent properties make imprinted Fe_3O_4 NPs to be for improving accessibility of the recognition cavities generated and separation efficiency of polymers from solution. Several protein molecularly imprinted works based on Fe_3O_4 NPs were reported, in which silane or other active groups (such as -C=C, -COOH, -CHO, and $-NH_2$) were introduced often involving harsh conditions and/or multiple functionalized steps.[21-23] Furthermore, the synthesis process was usually performed in organic solvents, which is a minus point for protein imprinting. Therefore, the requirements of more effective and simpler strategies for the protein imprinting on the surface of Fe_3O_4 NPs still exist. Our previous work[24] developed a much easier synthetic process for BHb imprinting employing amino group directly-functionalized Fe_3O_4 NPs as carriers. Though this work displayed some advantages in aspects of preparation technology, the hydrophilicity of the obtained products is unsatisfactory in virtue of adopting hydrophobic monomers.

Considering the solubility of protein, monomers with multifunctional groups and properties of hydrophilicity and biocompatibility are appropriate for imprinting proteins. Dopamine (DA), containing catechol and amine groups, is accepted to be a popular adhesive for protein.[25,26] The catechol groups are liable to be oxidized to generate o-quinone functionalities which make DA form thin polydopamine (PDA) films onto different kinds of materials in weak alkaline media at room temperature. To date, a certain number of successful examples using DA as monomer and cross-linker for protein imprinting have been reported.[27-29] However, to the best of our knowledge, adopting DA as monomer for imprinting of protein on the surface of amino group directly-functionalized Fe_3O_4 NPs has not been reported yet.

Taking into account the advantages of surface imprinting technology, magnetic separation, and PDA, the key idea of this work is to develop a facile approach to imprint protein on the surface of amino group directly-functionalized Fe_3O_4 NPs using dopamine as monomer through two-step immobilized template process. The procedure of this preparation method was rather green and simple. The obtained

nanomaterials could be easily separated from the solution under an external magnet within three seconds. In order to obtain the best recognition performance, the polymerization and adsorption conditions were investigated detailedly. In addition, practicability of the as-prepared imprinted polymers for biological application was further investigated by separation and removal of target protein from a real bovine blood sample. Furthermore, four other proteins with different isoelectric points were chosen as the templates to evaluate the versatility of the approach developed in this work.

2. Experiments

2.1. Materials

Dopamine (DA) was purchased from Alfa Aesar Chemical Company. 1,6-Diaminohexane (DAH), sodium acetate anhydrous (NaOAc), ferric chloride hexahydrate ($FeCl_3 \cdot 6H_2O$), ethylene glycol (EG), diethylene glycol (DEG), ethanol, trihydroxymethyl aminomethane (Tris), sodium dodecyl sulfonate (SDS), and acetic acid (HAc) were provided by Xi'an Chemicals Ltd. Bovine serum albumin (BSA; pI = 4.9, M_w = 66.0 KDa), bovine hemoglobin (BHb; pI = 6.9, M_w = 64.0 KDa), bovine pancreas ribonuclease A (RNase A; pI = 9.4, M_w = 13.7 KDa), hemoglobin (Hb; pI = 6.8, M_w = 65.0 KDa), transferrin (transferrin; pI = 5.5, M_w = 77.0 KDa), immunoglobulin G (IgG; pI = 8.0, M_w = 150 KDa), and lysozyme (Lyz; pI = 11.2, M_w = 13.4 KDa) were obtained from Sigma. The highly purified water (18.0 MΩ cm^{-1}) was prepared with a WaterPro water system (Axlwater Corporation, TY10AXLC1805-2, China) and used throughout the experiments. The bovine blood sample was kindly gifted from the local market. All reagents were of at least analytical grade and used without further treatment.

2.2. Preparation of Fe_3O_4@BSA-MIPs and Fe_3O_4@NIPs

The amino-modification Fe_3O_4 nanoparticles (denoted as Fe_3O_4@NH_2) were synthesized according to a previous method[30] with some modifications. $FeCl_3 \cdot 6H_2O$

(1.0 g), NaOAc (3.5 g), and DAH (6.0 g) were dissolved in a mixture of EG (10 mL) and DEG (10 mL) in a Teflon-lined stainless-steel autoclave, sealed to heat at 200 ^{o}C. After reaction for 8 h, the autoclave was cooled to room temperature. The resultant black products were washed with highly purified water and ethanol to remove the solvent and unreacted DAH, and then dried in vacuum for further use.

The optimal experimental conditions of polymerization of BSA surface-imprinted magnetic nanoparticles were carried out as follows: （1）The mass of immobilized template. BSA (10 mg, 20 mg, 30 mg, 40 mg, and 50 mg, respectively) was dissolved in 10 mM Tris-HCl buffer (pH = 8.5, 30 mL) in a three-neck round-bottom flask, and mixed with Fe_3O_4@NH_2 (200 mg). The mixture was stirred for 30 min to obtain Fe_3O_4@NH_2-BSA complex. The complex was collected by an external magnetic field and left in the bottom of the flask, and the concentration of BSA in the supernatant was detected by UV-vis spectrophotometer at about 280 nm. （2）The amount of functional monomer. DA (50 mg, 75 mg, 100 mg, 125 mg, and 150 mg, respectively) and 30 mL of Tris-HCl buffer (pH = 8.5, 10 mM) were added to the above flask, and stirred for 5 h at room temperature. The obtained products were rinsed with highly purified water until the supernatant was clear, and then washed with SDS-HAc (2%) to remove the template protein until no adsorption was detected by UV-vis spectrophotometer. The resulting imprinted polymers (denoted as Fe_3O_4@BSA-MIPs) were collected by an external magnetic field and washed with highly purified water, then dried under vacuum. Non-imprinted polymers (denoted as Fe_3O_4@NIPs) were prepared following the same procedure in the absence of the template protein BSA. Furthermore, the immobilization time of BSA and the polymerization time of DA were also investigated.

Moreover, to testify the efficiency of Fe_3O_4@NH_2 as the support, bare magnetic molecularly imprinted and non-imprinted polymers (denoted as B-Fe_3O_4@BSA-MIPs and B-Fe_3O_4@NIPs) were also prepared by the same way as that of Fe_3O_4@BSA-MIPs and Fe_3O_4@NIPs except for employing bare magnetic nanoparticles as the support.

2.3. Binding experiments

To investigate the kinetics adsorption of Fe_3O_4@BSA-MIPs and Fe_3O_4@NIPs, 10 mg of adsorbents were suspended in 10 mL of BSA Tris-HCl buffer (pH = 7.0, 10 mM) solution at a concentration of 0.30 mg mL^{-1}. The mixture was incubated at regular time intervals from 5 min to 60 min at room temperature, and the polymers were magnetically separated from the solution. Then, the concentration of BSA in the supernatant was measured by UV-vis spectrophotometer.

The adsorption capacity (Q) of the template protein or competitive protein bound to the imprinted polymers is calculated as follows:

$$Q = \frac{(C_0 - C_e)V}{m} \quad (1)$$

Where C_0 and C_e (mg mL^{-1}) represent the initial and the equilibrium solution concentration of the adsorbed protein, V (mL) represents the volume of the solution, and m (mg) is the weight of the imprinted polymers.

Isothermal adsorption experiment was operated through changing the concentrations of BSA from 0.050 to 0.50 mg mL^{-1} in Tris-HCl buffer (pH = 7.0, 10 mM) while employing 10 mg of Fe_3O_4@BSA-MIPs or Fe_3O_4@NIPs and shaking for 20 min at room temperature. Then, the adsorbents were isolated by a magnet and the residue BSA in the supernatant was determined by UV-vis spectrophotometer.

To evaluate the specific adsorption capability of the as-prepared polymers, 10 mg of Fe_3O_4@BSA-MIPs and Fe_3O_4@NIPs were incubated in 3 mL of Tris-HCl (10 mM, pH = 7.0) solution of BSA, BHb, transferrin, and IgG at a concentration of 0.30 mg mL^{-1} respectively at room temperature for 20 min, then the separation and determination procedures were conducted as described earlier in the kinetics adsorption experiments.

The imprinting factor (*IF*) and selectivity coefficient (*SC*) are usually used to determine the selectivity properties of the imprinted polymers towards the template protein and competitive protein. The *IF* and *SC* are calculated from the following equations:

$$IF = \frac{Q_{MIP}}{Q_{NIP}} \quad (2)$$

$$SC = \frac{IF_{TEM}}{IF_{COM}} \quad (3)$$

Where Q_{MIP} and Q_{NIP} (mg g^{-1}) represent the adsorption capacity of protein for Fe_3O_4@BSA-MIPs and Fe_3O_4@NIPs, IF_{TEM} and IF_{COM} are the imprinting factors of template protein and competitive protein.

To evaluate the amino groups of the Fe_3O_4@NH_2 could enhance the adsorption performance of the imprinted nanoparticles, we compared the binding capabilities of Fe_3O_4@BSA-MIPs, Fe_3O_4@NIPs, B-Fe_3O_4@BSA-MIPs, and B-Fe_3O_4@NIPs. In detail, 10 mg of the above four polymers were incubated with 10 mL of BSA solution at a concentration of 0.30 mg mL^{-1} (pH = 7.0, 10 mM Tris-HCl) at room temperature for 20 min, respectively. Then, the extraction and detection procedures were conducted as described earlier in the adsorption experiments.

2.4. Reusability of resultant imprinted nanomaterials

To estimate the reusability of Fe_3O_4@BSA-MIPs and Fe_3O_4@NIPs, BSA adsorption-regeneration procedure was repeated 6 times by using the same polymers. Briefly, 10 mg of polymers were added to 10 mL of BSA solution at a concentration of 0.30 mg mL^{-1} (pH = 7.0, 10 mM Tris-HCl) and incubated at room temperature for 20 min. Then, Fe_3O_4@BSA-MIPs or Fe_3O_4@NIPs were removed by a magnet and the bound amount of BSA was quantified by UV-vis spectrophotometer. The reused polymers were eluted with SDS-HAc (2%) for 3 h to ensure complete removal of the adsorbed BSA. The recovered products were then reused for adsorption of BSA for another 5 cycles, and every cycle of supernatant was collected and determined by UV-vis spectrophotometer at about 280 nm.

2.5. Real sample analysis

10 mg of Fe_3O_4@BSA-MIPs were merged with 10 mL of the standard protein mixture (containing 0.30 mg mL^{-1} BSA and 0.30 mg mL^{-1} BHb) and bovine blood

sample diluted 150-fold with Tris-HCl buffer solution (pH = 7.0, 10 mM), respectively. After incubation for 20 min under gentle shaking, SDS-HAc (2%) was employed to elute the adsorbed protein for 3 h. The diluted, adsorbed, and eluted samples were used for SDS-PAGE analysis.

2.6. Versatility investigation

The versatility of this approach was evaluated by using another three magnetic imprinted polymers generated in the same way as that of Fe_3O_4@BSA-MIPs except for adopting BHb, Hb, RNase A, and Lyz as the template protein respectively, which were denoted as Fe_3O_4@BHb-MIPs, Fe_3O_4@Hb-MIPs, Fe_3O_4@RNase A-MIPs, and Fe_3O_4@Lyz-MIPs. The full cross-reaction characterizations of four protein-imprinted nanomaterials along with non-imprinted Fe_3O_4@NIPs were investigated by adsorbing corresponding template protein and three other proteins, namely, 10 mg of polymers were incubated with 10 mL of Tris-HCl buffer (pH = 7.0, 10 mM) solution of BSA, BHb, Hb, RNase A, and Lyz at a concentration of 0.30 mg mL^{-1} respectively at room temperature for 20 min. Then, the extraction and detection procedures were conducted as described earlier in the binding experiments.

2.7. Characterization

The morphology of the obtained nanomaterials was studied using a Tecnai G2 T2 S-TWIN transmission electron microscope (TEM). Fourier transform infrared (FT-IR) spectra were obtained *via* a Nicolet AVATAR 330 FT-IR spectrophotometer. The identification of the crystalline phase was carried out by a Rigaku D/max/2500v/pc (Japan) X-ray diffractometer with Cu Kα radiation. The magnetic properties were analyzed with a vibrating sample magnetometer (VSM) (LDJ 9600-1, USA). The data of adsorption were measured by using a UV-2450 spectrophotometer (Shimadzu, Japan). Electrophoretic analysis of protein samples was performed using regular SDS-PAGE (Bio-Rad, Hercules, CA) with 10% running and 5% stacking gels. Proteins were stained with Coomasie Brilliant Blue R-250.

3. Results and discussion

3.1. Preparation of Fe_3O_4@BSA-MIPs

The procedure for the preparation of Fe_3O_4@BSA-MIPs, combining the merits of surface imprinting technology, two-step immobilized template strategy, functionalized magnetic nanomaterials, and hydrophilicity of DA, was displayed in Fig. 1. First, the Fe_3O_4@NH_2 whose surface were full of numerous amino groups was synthesized through a modified one-step solvothermal method, using $FeCl_3 \cdot 6H_2O$ as a single iron source and DAH as ligand. Next, the template protein BSA was immobilized on the surface of Fe_3O_4@NH_2 through multi-hydrogen interaction between the amino groups of Fe_3O_4@NH_2 and the amino acids on BSA to form Fe_3O_4@NH_2-template complex. Then, a thin adherent polydopamine (PDA) shell was deposited on the surface of Fe_3O_4@NH_2 to further immobilize the template protein by using DA as the monomer and crosslinker. Notely, the dopamine units possess amino, hydroxyl, and phenyl groups which can interact with BSA through multi-hydrogen bonds and hydrophobic effect. The two immobilized template processes can orientate template proteins orderly and have the imprinted sites uniformed for improving the imprinting effect.[31] Finally, after washing with the 2% SDS-HAc solution, the Fe_3O_4@BSA-MIPs with imprinted recognition sites complementary to BSA in shape, size, and functional group orientation were obtained.

/Fig. 1/

3.2. Optimization of polymerization conditions

When we carried out the optimal experimental conditions, the effect of different mass of immobilization of BSA onto Fe_3O_4@NH_2 in the range of 10-50 mg was investigated. As shown in Table S1, the Q_{IM} increased with the increasing of Q_{AD} from 10 mg to 30 mg, indicating that a higher Q_{AD} might make Fe_3O_4@NH_2 interact adequately with BSA through forming multi-hydrogen. However, the Q_{IM} remained almost unchanged with the increasing of Q_{AD} from 30 mg to 50 mg. The possible reason was that the amounts of amino groups of Fe_3O_4@NH_2 had been saturated with BSA. Excessive Q_{AD} could not increase the immobilization. Thus, the Q_{AD} of 30 mg

was chosen in the work. Furthermore, we also evaluated the immobilization time of BSA varying from 10 min to 50 min. The results were presented in Table S2, from which we could find that the best immobilization time was 30 min.

To optimize recognition performance of Fe_3O_4@BSA-MIPs, the thickness of the PDA shell which is controlled by the amount of DA was adjusted from 50 mg to 150 mg. The results of the adsorption capacity (*Q*) and imprinting factor (*IF*) were presented in Fig. 2A. Both *Q* and *IF* increased with the increasing of the amount of DA from 50 mg to 100 mg, indicating that enough functional monomers could react adequately with template proteins and create enough number of recognition cavities in the network of polymers to enhance the imprinting ability of the Fe_3O_4@BSA-MIPs towards BSA. However, a decrease of *Q* and *IF* was observed when the amount of DA was further increased. Too thick PDA imprinted shells may make it hard for protein to access to the recognition cavities. Therefore, the amount of DA of 100 mg was chosen for the polymerization of Fe_3O_4@BSA-MIPs in accordance with the experimental results.

The polymerization time of DA was adjusted varying from 3 h to 7 h to seek the shortest experimental period and the best binding performance. The results were displayed in Fig. 2B. It is indicated that the optimal recognition sites and the most suitable shell thickness were formed when the polymerization time was 5 h. The polymerization degree was incompleted when the polymerization time was less 5 h, because the thin PDA shell only could immobilize less template and crate less imprinted cavities. Conversely, too many monomers self-polymerized to block the recognition sites, and impacted the imprinted effect of the polymers when the polymerization time was over 5 h. Therefore, 5 h was chosen as the polymerization time in this work.

/Fig. 2/

3.3. Characterization of obtained nanomaterials

The morphological structure and size of Fe_3O_4@NH_2 and Fe_3O_4@BSA-MIPs were characterized by TEM. As can be seen from Fig. 3, the obtained nanomaterials

revealed spherical structure with a narrow particle size distribution. Through the statistic analysis of particles, the average diameter of Fe_3O_4@NH_2 (Fig. 3A) was about 60 nm. It was found that the Fe_3O_4@BSA-MIPs with distinguishable core-shell structure were successfully prepared after two-step template immobilization process, and whose diameter increased to approximately 80 nm (Fig. 3B), indicating that the thickness of the PDA imprinting shell was just about 10 nm. The thickness was suitable for the three-dimensional structure of the BSA,[32] making the mass transport between solution and the surface of Fe_3O_4@BSA-MIPs easier.

/Fig. 3/

The chemical groups for the pristine Fe_3O_4@NH_2 and Fe_3O_4@BSA-MIPs (Fig. 4) were characterized by FT-IR spectra. The strong peak at 575 cm^{-1} observed in both samples (curve a and b) was attributed to the stretch of the Fe-O vibration. The peaks at around 1080 cm^{-1} and 1640 cm^{-1}corresponding to the C-N stretch and bending vibration of N-H[24] respectively, indicate that the amino functionalization was on the surface of Fe_3O_4@NH_2 (curve a). When compared with Fe_3O_4@NH_2, the new appearance of typical peaks in the spectra of Fe_3O_4@BSA-MIPs (curve b), such as phenylic C=C stretching at 1500 cm^{-1}, the enhanced adsorption peak intensity of C-N bond at 1640 cm^{-1}, and the lessened characteristic peak of Fe-O bond at 575 cm^{-1} should be attributed to the coating of PDA layer on the magnetic nanoparticles.

/Fig. 4/

The crystalline structure of Fe_3O_4@NH_2 and Fe_3O_4@BSA-MIPs was characterized by XRD in the 2θ range of 20º-70º (Fig.5). Six characteristic peaks of Fe_3O_4 (2θ = 30.38º, 35.58º, 43.14º, 53.48º, 57.08º, and 62.66º) were observed from both two samples. The peak positions at the corresponding 2θ values were indexed as (220), (311), (400), (422), (511), and (440), respectively, which matched well with the database of magnetite in the JCPDS-International Center for Diffraction Data (JCPDS Card: 19-629). The distinctive diffraction peaks of Fe_3O_4@BSA-MIPs were in agreement with those of Fe_3O_4, illustrating that the obtained imprinted

polymers containing Fe_3O_4 with a spinel structure and the phase of Fe_3O_4 did not result in changing in the process of synthesis.[33]

/Fig. 5/

The magnetic properties of the Fe_3O_4@NH_2 and core-shell Fe_3O_4@BSA-MIPs were studied using a vibrating sample magnetometer at room temperature. Fig. 6 illustrated the plots of magnetization *versus* magnetic field (*M-H* loop) of Fe_3O_4@NH_2 (curve a) and Fe_3O_4@BSA-MIPs (curve b) from which could find there were no remanence and coercivity, demonstrating that both polymers were superaramagnetic. It is noteworthy that the saturation magnetization of Fe_3O_4@BSA-MIPs (40.7 emu g^{-1}) was lower than that of Fe_3O_4@NH_2 (53.5 emu g^{-1}), which was ascribed to the shielding effect of PDA shell on the surface of Fe_3O_4@NH_2. The experimental results display that the obtained imprinted polymers possess sufficient magnetic force to be separated fast from the solution under an external magnet within three seconds.

/Fig. 6/

3.4. Adsorption performance

3.4.1. Adsorption kinetics

Adsorption kinetics of BSA onto Fe_3O_4@BSA-MIPs and Fe_3O_4@NIPs were investigated, and the curves of binding capacity *versus* time were presented in Fig. 7 A. It could be observed that the increase of the adsorption capacity of BSA onto Fe_3O_4@BSA-MIPs was quite fast within the first 10 min, and then almost reached equilibrium after 20 min. The adsorption equilibrium time of the obtained nanomaterials was shorter than that of some other surface imprinting polymers for BSA.[34,35] The rapid adsorption rate towards BSA due to the large surface-to-volume ratios of the carriers and the thin imprinting shells, which made BSA approach the binding sites easily with lower mass-transfer resistance. It was also noted that the Fe_3O_4@BSA-MIPs had much higher adsorption capacity than that of Fe_3O_4@NIPs, suggesting the favorable recognition performance of resultant imprinted

nanomaterials.

To further investigate the kinetic mechanisms of adsorption, the obtained data were calculated by the second-order rate equation that be expressed as follows :

$$\frac{t}{Q_t} = \frac{1}{KQ_e^2} + \frac{t}{Q_e} = \frac{1}{v_0} + \frac{t}{Q_e} \quad (4)$$

Where Q_e and Q_t (mg g^{-1}) are the amounts of BSA adsorbed onto Fe_3O_4@BSA-MIPs or Fe_3O_4@NIPs at the equilibrium and at time t (min), respectively; K (g mg^{-1} min^{-1}) represents the rate constant of the second-order adsorption; v_0 (mg g^{-1} min^{-1}) is the initial adsorption rate.

As shown in Table 1, the correlation coefficients (r) of Fe_3O_4@BSA-MIPs and Fe_3O_4@NIPs are 0.9998 and 0.9964, indicating that the second-order model fitted the binding data well. The values of v_0 implied that the initial adsorption rate of Fe_3O_4@BSA-MIPs was much faster than that of Fe_3O_4@NIPs, which was in keeping with Fig. 7A. The results also illustrated that the adsorption capacity was proportional to the number of active recognition sites on the surface of the imprinted nanomaterials, and the chemical adsorption was the rate-limiting step in the recognition process of the resulting polymers.[36]

3.4.2. Adsorption isotherms

The adsorption isothermal experiments were performed at different initial concentrations of BSA, ranging from 0.050 to 0.50 mg mL^{-1} (Fig. 7B). As the isothermal curves shown, the amount of BSA bound to the Fe_3O_4@BSA-MIPs and Fe_3O_4@NIPs increased quickly along with increasing the initial concentration of BSA and then reached saturation when the concentration was above 0.30 mg mL^{-1}. The experimental maximum adsorption capacity of BSA onto Fe_3O_4@BSA-MIPs (107.8 mg g^{-1}) was 3.35 times higher than that of Fe_3O_4@NIPs (32.15 mg g^{-1}). Large amount of specific recognition cavities on Fe_3O_4@BSA-MIPs results in a higher affinity towards BSA than that of non-imprinted nanomaterials. Furthermore, compared with some other works for surface imprinting BSA using Fe_3O_4 as the support, the binding amount in this work was much higher,[22,32] confirming that DA, possessing favorable

hydrophilicity and abundant functional groups, could create more imprinted sites which fitted well with template protein in the water-solubility, chemical effect, and steric structure.

The saturation binding data was further processed by the Freundlich and Langmuir isothermal models to estimate the adsorption properties of the resultant nanomaterials. The two models are expressed as follows:

$$\log Q = \log K_F + n \log C_e \quad (5)$$

$$\frac{C_e}{Q} = \frac{1}{Q_{max} K_L} + \frac{C_e}{Q_{max}} \quad (6)$$

Where Q (mg g^{-1}) is the amount of BSA bound to Fe_3O_4@BSA-MIPs at equilibrium, Q_{max} (mg g^{-1}) is the apparent maximum adsorption capacity, C_e (mg mL^{-1}) is the free analytical concentration at equilibrium, K_L and K_F (mL mg^{-1}) are the Langmuir and Freundlich constant respectively, and n is the Freundlich exponent which represents the heterogeneity of the system. The values of K_L, Q_{max} and n, K_F can be calculated from the slope and intercept of the linear plotted in C_e/Q *versus* C_e and log Q *versus* log C_e, respectively.

Langmuir isotherm model is assumed that the adsorption takes place at specific homogeneous sites as well as monolayer sorption, and each site can bind only one molecule.[37] While the Freundlich isotherm model is applied to multi-layer adsorption and unfavorable adsorption on heterogeneous surfaces.[38] Through comparison of r values displayed in Table 1, we can conclude that the experimental data are better fitted with the Langmuir isotherm model ($r > 0.99$) than Freundlich model ($r < 0.94$). The maximum adsorption capacities obtained from experiment are also close to the apparent maximum adsorption capacities (117.6 mg g^{-1} for Fe_3O_4@BSA-MIPs and 39.37 mg g^{-1} for Fe_3O_4@NIPs) calculated using the Langmuir isotherm model. In light of the results, the binding of BSA onto the resultant nanomaterials may be all monolayer adsorption, and no further binding could take place at the binding site once a template molecule occupied this site.

/Fig. 7/

/Table 1/

3.4.3. Comparison of two kinds of imprinted nanoparticles

The adsorption performances of B-Fe_3O_4@BSA-MIPs and B-Fe_3O_4@NIPs were also investigated. The results of the comparison of two kinds of imprinted nanomaterials prepared adopting different supports were presented in Table 2. It is obvious that the binding amount of B-Fe_3O_4@NIPs was close to that of Fe_3O_4@NIPs. However, the adsorption capacities showed a great difference between Fe_3O_4@BSA-MIPs and B-Fe_3O_4@BSA-MIPs. Fe_3O_4@BSA-MIPs had a much higher binding amount and imprinting factor, twice as much as those of B-Fe_3O_4@NIPs, demonstrating that the amino groups played an important role in the process of protein recognition. Because Fe_3O_4@BSA-MIPs were obtained by "template immobilization strategy", the -NH_2 on the surface of Fe_3O_4@NH_2 could orientate the template proteins in an orderly fashion and create more homogenous binding sites in the polymer matrix.

/Table 2/

3.4.4. Specificity

BHb, IgG, and transferrin were chosen as competitive proteins to illustrate the recognition specificity of the imprinted nanomaterials for template BSA due to the following reasons. (1) BHb is another high-abundant protein in the bovine blood serum and has similar molecular volume and weight with BSA; (2) IgG and transferrin are proteins which have relatively lower quantities in the blood. The adsorption of Fe_3O_4@BSA-MIPs and Fe_3O_4@NIPs to BSA, BHb, IgG, and transferrin with a concentration of 0.30 mg mL^{-1} in 3 mL of Tris-HCl buffer were examined, respectively (Fig. 8A and Table S3). Obviously, the imprinted polymers exhibited a much higher binding amount for template protein BSA than those of BHb, IgG, and transferrin. However, the adsorption capacity of BSA for Fe_3O_4@NIPs was quite close to those of three other competitive proteins. The difference suggested that the specific recognition cavities complementary in shape, size, and functional groups with

template protein were formed in the thin imprinting PDA shells of Fe_3O_4@BSA-MIPs. Moreover, the imprinting factor of BSA (3.35) was higher than those of BHb (1.97), IgG (1.19), and transferring (1.21). These results further proved the excellent imprinting efficiency of the present method.

3.5. Reusability

The property of reusability is of significance for actual application of polymers. To testify the stability of the prepared magnetic nanomaterials, the adsorption-regeneration cycle was repeated six times by using the same Fe_3O_4@BSA-MIPs and Fe_3O_4@NIPs. As shown in Fig. 8B, the adsorption capacity of Fe_3O_4@BSA-MIPs lost only 7.1% after six cycles, which might be because some recognition cavities of imprinted polymers were clogged after regeneration or destroyed after washing, and thus, they were no longer fit for the template molecules. Whereas, the affinity of Fe_3O_4@NIPs remained almost unchanged, because whose recognition was nonspecific and the effect of washing could be ignored. After adsorption-regeneration for six times, the adsorption performance of the imprinted and non-imprinted magnetic nanomaterials prepared in this work were stable, which is an outstanding advantage for practical application.

/Fig. 8/

3.6. Application

Serum albumin accounts for approximately 50% of total blood plasma proteins,[39] which is considered as a shelter in the analysis of biomarkers that are commonly at lower concentration levels in plasma sample. Therefore, we chosen the fresh bovine blood diluted 150-fold with Tris-HCl (pH = 7.0, 10 mM) as the real sample to further evaluate the practicability of Fe_3O_4@BSA-MIPs. The SDS-PAGE analysis is illustrated in Fig. 9. There were two bands in the Lane 1, indicating the mixture of BSA and BHb. It was found from lane 2 that the band of BSA faded apparently after treatment with Fe_3O_4@BSA-MIPs, while the band of BHb had little change. The BSA band was reappeared in Lane 3 after elution with 2% SDS-HAc solution, revealing

that the BSA was selectively captured by Fe_3O_4@BSA-MIPs. Lane 5 displayed the supernatant of the fresh bovine blood diluted 150-fold (Lane 4) after treatment with Fe_3O_4@BSA-MIPs, in which almost BSA was disappeared while other bands were reserved, suggesting that Fe_3O_4@BSA-MIPs had specific recognition for BSA in the bovine blood sample and less co-adsorption with others. After elution with 2% SDS-HAc solution, only the band of BSA was observed (Lane 6), indicating that the BSA was selectively isolated and recovered from the real sample after elution. The above results confirmed that the specificity and practicability of Fe_3O_4@BSA-MIPs for the separation of BSA.

/Fig. 9/

3.7. Method validation

The generality of the proposed imprinting approach was further investigated through the full cross-selectivity test of four protein-imprinted nanomaterials along with non-imprinted Fe_3O_4@NIPs, and the results are summarized in Table 3. It was clearly observed that the adsorption capacity, imprinting factor, and selectivity coefficient of different imprinted polymers to corresponding template proteins were all higher than those of the three other proteins, demonstrating that the developed method was valid to imprint different kinds of proteins with different isoelectric points. It is worth mentioning that BHb-imprinted nanomaterials in this work have a larger adsorption capacity (181.1 mg g^{-1}) towards BHb and a higher imprinting factor (4.96) than those of our previous work (37.58 mg g^{-1}, 3.60)[24]. The greatest difference lies in that the latter adopted two types of silane coupling agent as monomers while the former employed DA as monomer. It is also worth noting that Hb-imprinted nanoparticles in this work have a considerable large adsorption capacity (187.9 mg g^{-1}) towards Hb and a relatively higher imprinting factor (5.48) than those of zhou's work (17.50 mg g^{-1}, 5.01).[20] The main contrast was that the latter employed bare Fe_3O_4 nanoparticles as support while the former used Fe_3O_4@NH_2 instead. Therefore, NH_2-modification on the surface of Fe_3O_4 nanoparticles would enhance the performance of the imprinted nanomaterials.

/Table 3/

4. Conclusion

In this work, a facile, general, and economical approach was successfully developed to imprint protein on the surface of Fe_3O_4@NH_2 using dopamine as monomer. Because of combining the advantages of surface imprinting technology, immobilized template strategy, magnetic separation, and PDA, these resulting imprinted nanomaterials exhibited fast kinetics, large adsorption capacity, high selectivity, and satisfactory reusability. Furthermore, the favorable versatility for proteins with different isoelectric points, and the successful applications in the specific capture of the target protein from a real sample of bovine blood and good recovery after a reasonably mild elution, indicating that the proposed method could be expected to be an alternative solution for selective removal of high-abundant proteins from complex biological samples.

Acknowledgements

The authors are grateful for financial support from the National Natural Science Foundation of China (No. 21305107), the Fundamental Research Funds for the Central Universities (Nos. 08143081, 08142034), and China Postdoctoral Science Foundation (No. 2014M562388).

References

1. F. R. Wang, C. Chmil, F. Pierce, K. Ganapathy, B. B. Gump, J. A. MacKenzie, Y. Mechref and K. Bendinskas, *J. Chromatogr. B* 2013, **934**, 26-33.
2. J. L. Cao, X. H. Zhang, X. W. He, L. X. Chen and Y. K. Zhang, *J. Mater. Chem. B* 2013, **1**, 3625-3632.
3. M. Javanmard, S. Emaminejad, C. Gupta, J. Provine, R. W. Davis and R. T. Howe, *Sensors Actuat. B- Chem*. 2014, **193**, 918-924.
4. M. Javanmard, S. Emaminejad, R. W. Dutton and R. W. Davis, *Anal. Chem*. 2012, **84**, 1432-1438.
5. D. N. Gunasena and Z. El Rassi, *J. Sep. Sci*. 2011, **34**, 2097-2105.

6. R. L. Gundry, M. Y. White, J. Nogee, I. Tchernyshyov and J. E. Van Eyk, *Proteomics* 2009, **9**, 2021-2028.
7. B. Li, J. J. Xu, A. J. Hall, K. Haupt and B. Tse Sum Bui, *J. Mol. Recognit.* 2014, **27**, 559-565.
8. A. Mirmohseni, M. Shojaei and R. Pourata, *RSC Adv*. 2014, **4**, 20177-20184.
9. E. Yildirim, E. Turan and T. Caykara, *J. Mater. Chem.* 2012, **22**, 636-642.
10. K. El Kirat, M. Bartkowski and K. Haupt, *Biosens. Bioelectron.* 2009, **24**, 2618-2624.
11. J. Bognár, J. Szücs, Z. Dorkó, V. Horváth and R. E. Gyurcsányi, *Adv. Funct. Mater.* 2013, **23**, 4703-4709.
12. T. Wangchareansak, C. Sangma, K. Choowongkomon, F. Dickert and P. Lieberzeit, *Anal. Bioanal. Chem.* 2011, **400**, 2499-2506.
13. M. Bosserdt, N. Gajovic-Eichelman and F. W. Scheller, *Anal. Bioanal. Chem*. 2013, **405**, 6437-6444.
14. A. M. Bossi, P. S. Sharma, L. Montana, G. Zoccatelli, O. Laub and R. Levi, *Anal*. *Chem*. 2012, **84**, 4036-4041.
15. V. Saumya, K. P. Prathish and T. P. Rao, *Talanta* 2011, **85**, 1056-1062.
16. L. Uzun, R. Uzek, S. Şenel, R. Say and A. Denizli, *Mater*. *Sci*. *Eng. C* 2013, **33**, 3432-3439.
17. F. Kartal and A. Denizli, *J. Sep. Sci.* 2014, **37**, 2077-2086.
18. E. Moczko, A. Guerreiro, E. Piletska and S. Piletsky, *Langmuir* 2013, **29**, 9891-9896.
19. R. X. Gao, X. R. Mu, J. J. Zhang and Y. H. Tang, *J. Mater*. *Chem*. *B* 2014, **2**, 783-792.
20. W. H. Zhou, C. H. Lu, X. C. Guo, F. R. Chen, H. H. Yang and X. R. Wang, *J. Mater. Chem.* 2010, **20**, 880-883.
21. W. W. Huang, X. Yang, S. Zhao, M. Zhang, X. L. Hu, J. Wang and H. T. Zhao, *Analyst* 2013, **138**, 6653-6661.
22. X. J. Li, B. L. Zhang, L. Tian, W. Li, T. J. Xin, H. P. Zhang and Q. Y. Zhang, *Sensors Actuat*. *B-Chem*. 2014, **196**, 265-271.
23. T. Jing, H. R. Du, Q. Dai, H. Xia, J. W. Niu, Q. L. Hao, S. R. Mei and Y. K. Zhou, *Biosens*. *Bioelectron*. 2010, **26**, 301-306.
24. R. X. Gao, X. R. Mu, Y. Hao, L. L. Zhang, J. J. Zhang and Y. H. Tang, *J. Mater*. *Chem*. *B* 2014, **2**, 1733-1741.
25. Y. Zhang, K. Panneerselvam, R. Ogaki, L. Hosta-Rigau, R. V. D. Westen, B. E. B. Jensen, B. M. Teo, M. F. Zhu and B. Städler, *Langmuir* 2013, **29**, 10213-10222.
26. A. Nematollahzadeh, A. Shojaei, M. J. Abdekhodaie and B. Sellergren, *J. Colloid Interf. Sci*. 2013, **404**, 117-126.

27. A. Tretjakov, V. Syritski, J. Reut, R. Boroznjak, O. Volobujeva and A. Öpik, *Microchim. Acta* 2013,**180**, 1433-1442.

28. 28. Z. W. Xia, Z. A. Lin, Y. Xiao, L. Wang, J. N. Zheng, H. H. Yang and G. N. Chen, *Biosens. Bioelectron*. 2013, **47**, 120-126.

29. R. Liu, M. Sha, S. S. Jiang, J. Luo and X. Y. Liu, *Talanta* 2014, **120**, 76-83.

30. L. Y. Wang, J. Bao, L. Wang, F. Zhang and Y. D. Li, *Chem. Eur. J*. 2006, **12**, 6341-6347.

31. L. J. Liu, J. J. Zheng, G. J. Fang and W. H. Xie, *Anal. Chim. Acta* 2012, **726**, 85-92.

32. X. J. Li, B. L. Zhang, W. Li, X. F. Lei, X. L. Fan, L. Tian, H. P. Zhang and Q. Y. Zhang, *Biosens. Bioelectron*. 2014, **51**, 261-267.

33. F. X. Chen, S. L. Xie, J. H. Zhang and R. Liu, *Mater. Lett*. 2013, **112**, 177-179.

34. D. R. Kryscio and N. A. Peppas, *Anal. Chim. Acta* 2012, **718**, 109-115.

35. M. S. Zhang, J. R. Huang, P. Yu and X. Chen, *Talanta* 2010, **81**, 162-166.

36. I. Koç, G. Baydemir, E. Bayram, H. Yavuz and A. Denizli, *J. Hazard. Mater*. 2011, **192**, 1819-1826.

37. S. Y. Tao, C. Wang, W. Ma, S. Wu and C. G. Meng, *Micropor. Mesopor. Mat*. 2012, **147**, 295-301.

38. R. Dan, Y. Z. Wang, L. Du, S. H. Du, M. D. Huang, S. Yang and M. Zhang, *Analyst* 2013, **138**, 3433-3443.

39. M. A. O. da Silva and M. A. Z. Arruda, *Talanta* 2009, **77**, 985-990.

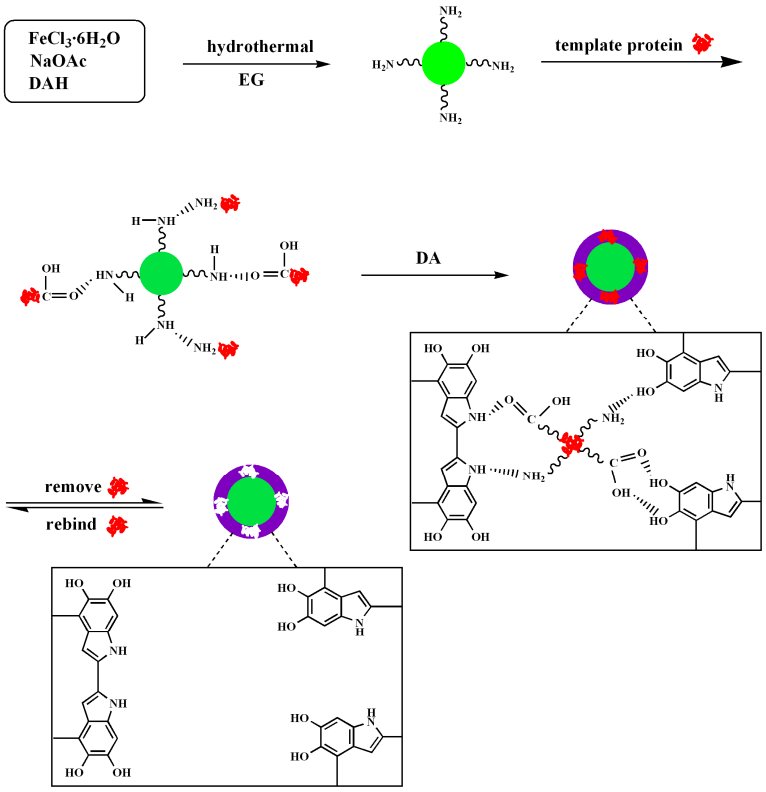

Fig. 1. The synthetic procedure of Fe_3O_4@BSA-MIPs.

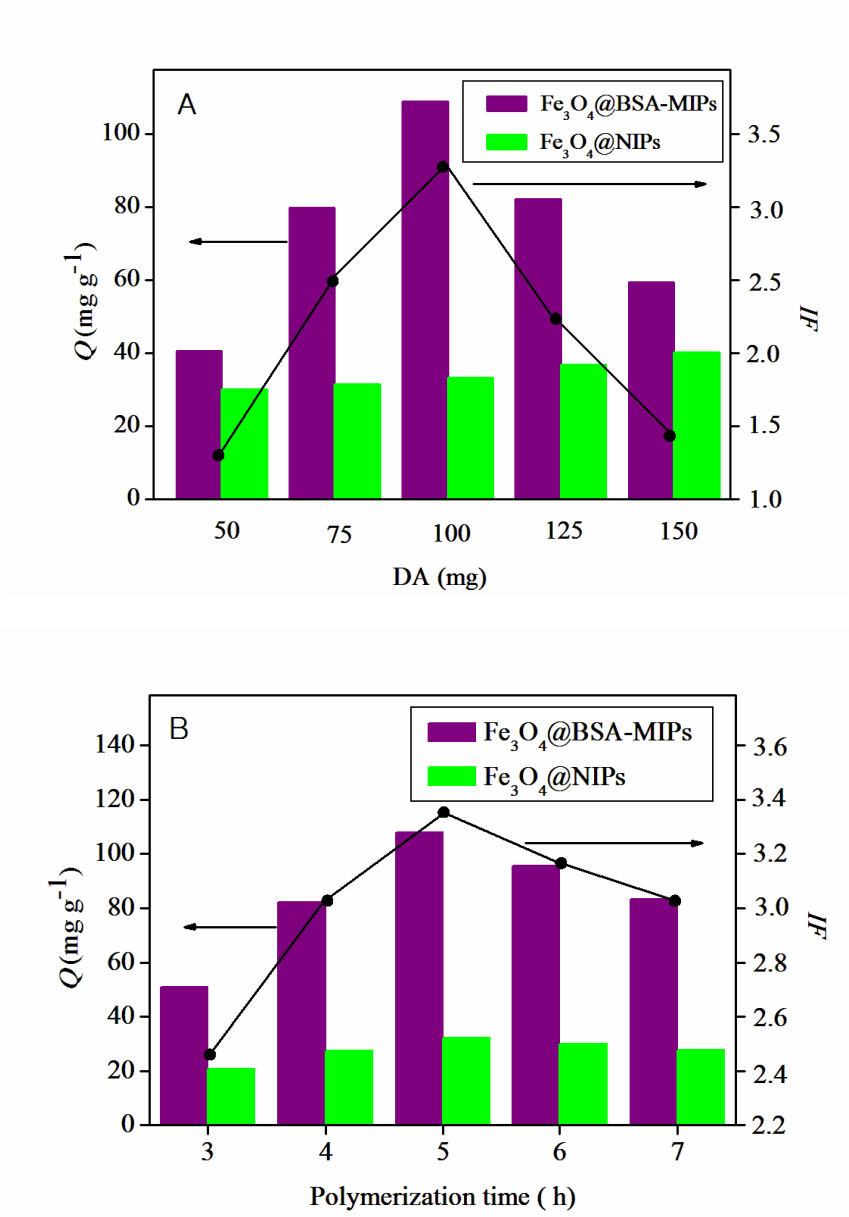

Fig. 2. Effect of the amount (A) and polymerization time (B) of DA on the imprinting performance of Fe_3O_4@BSA-MIPs and Fe_3O_4@NIPs.

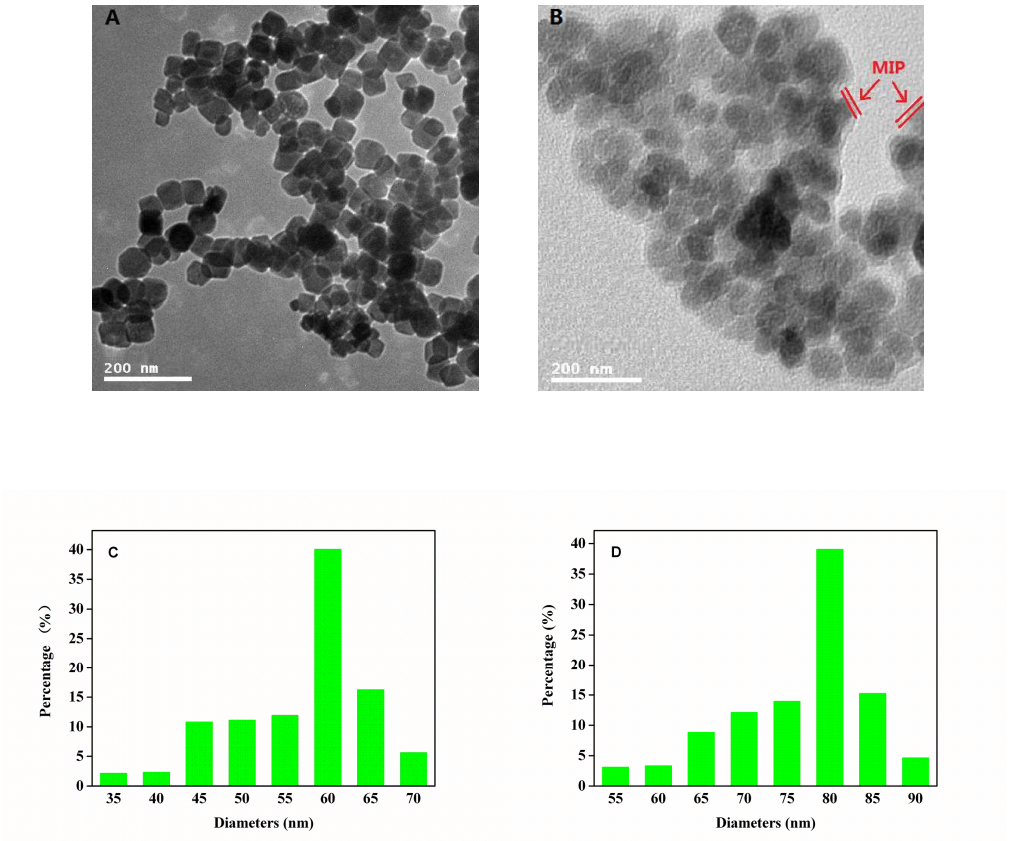

Fig. 3. TEM images of Fe_3O_4@NH_2 (A) and Fe_3O_4@BSA-MIPs (B);

the size distribution histograms of Fe_3O_4@NH_2 (C) and Fe_3O_4@BSA-MIPs (D).

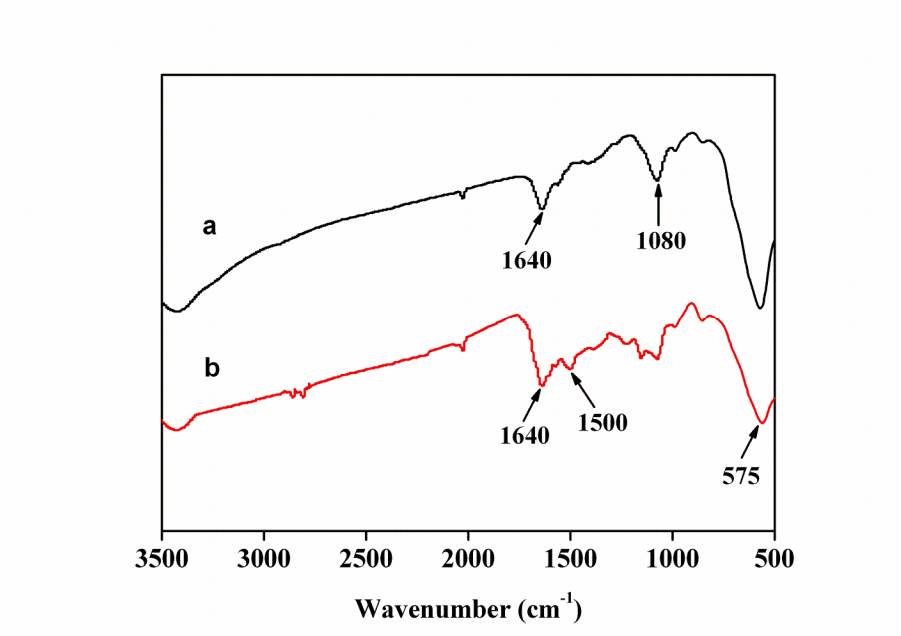

Fig. 4. FT-IR spctra of Fe_3O_4@NH_2 (a) and Fe_3O_4@BSA-MIPs (b).

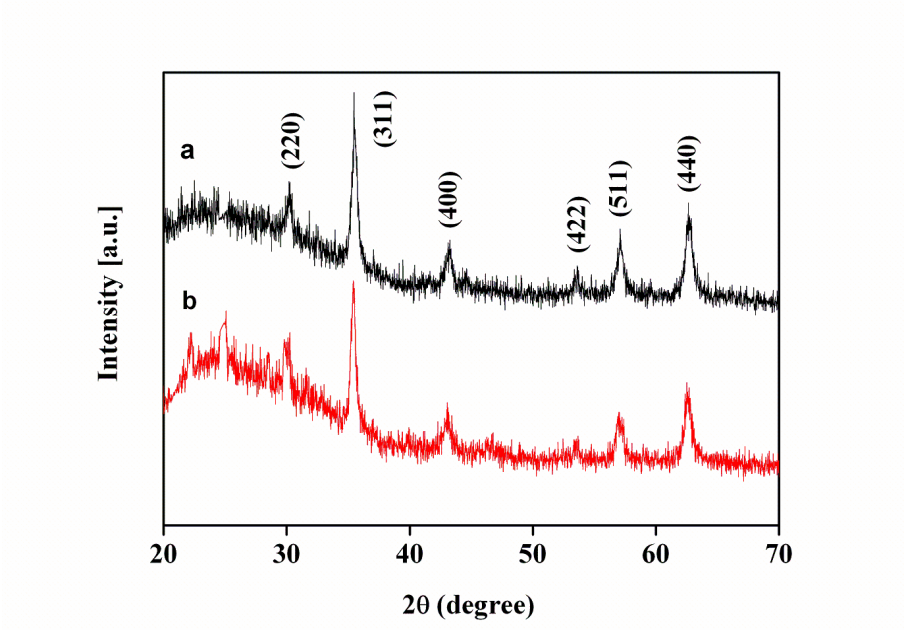

Fig. 5. XRD patterns of Fe_3O_4@NH_2 (a) and Fe_3O_4@BSA-MIPs (b).

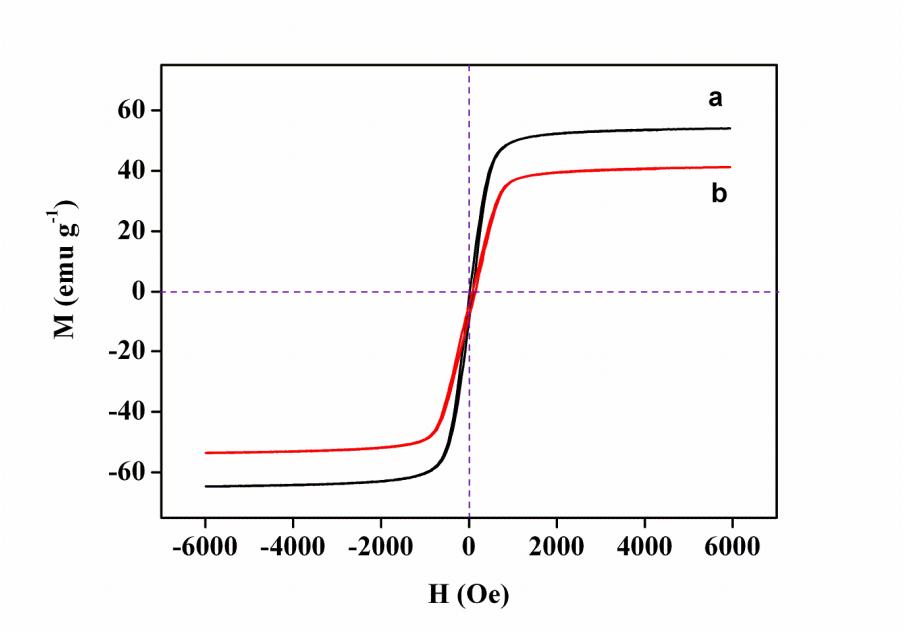

Fig. 6. Magnetization curves of Fe_3O_4@NH_2 (a) and Fe_3O_4@BSA-MIPs (b).

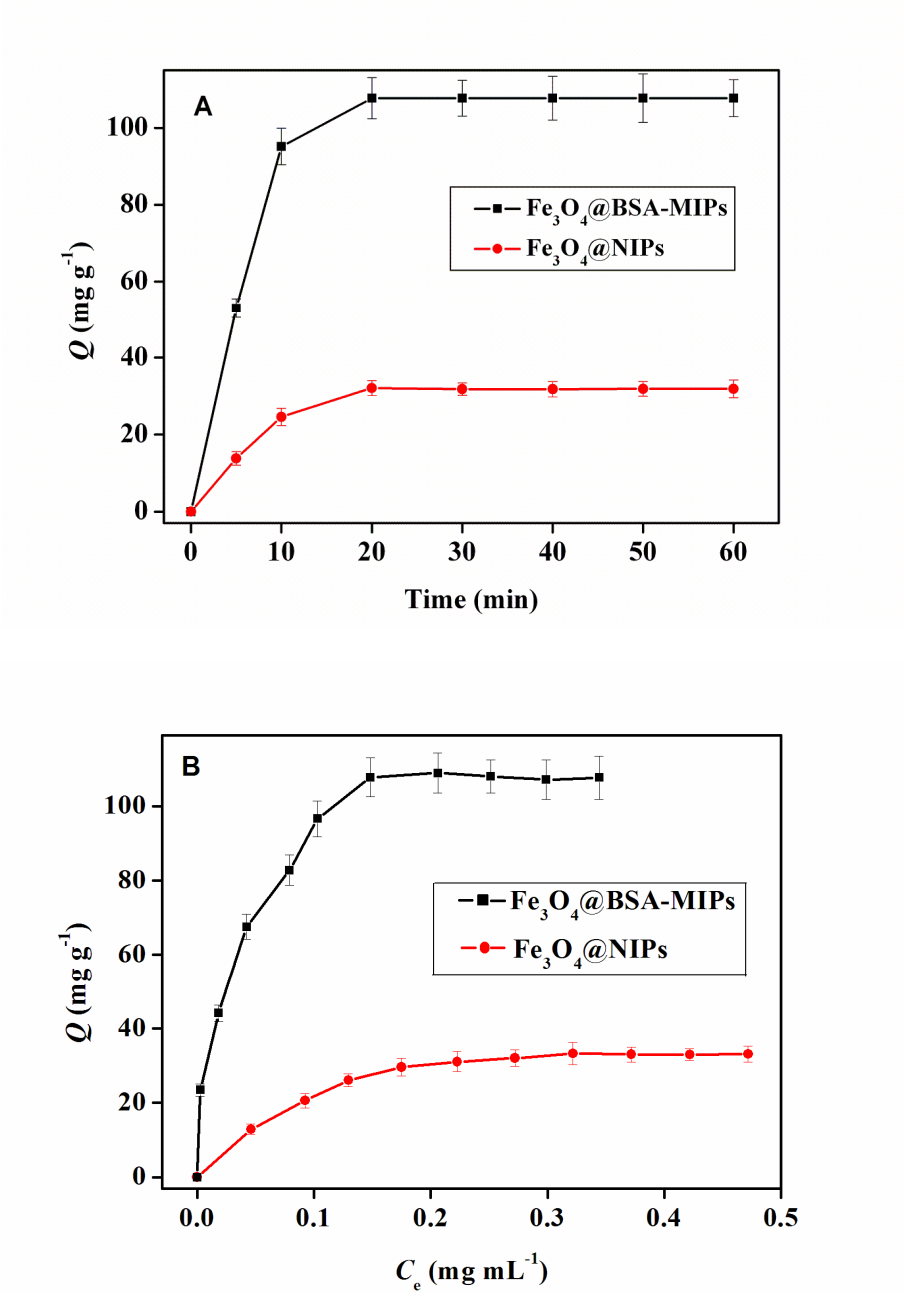

Fig. 7. Adsorption kinetics (A) and isotherms (B) of BSA onto Fe_3O_4@BSA-MIPs and Fe_3O_4@NIPs.

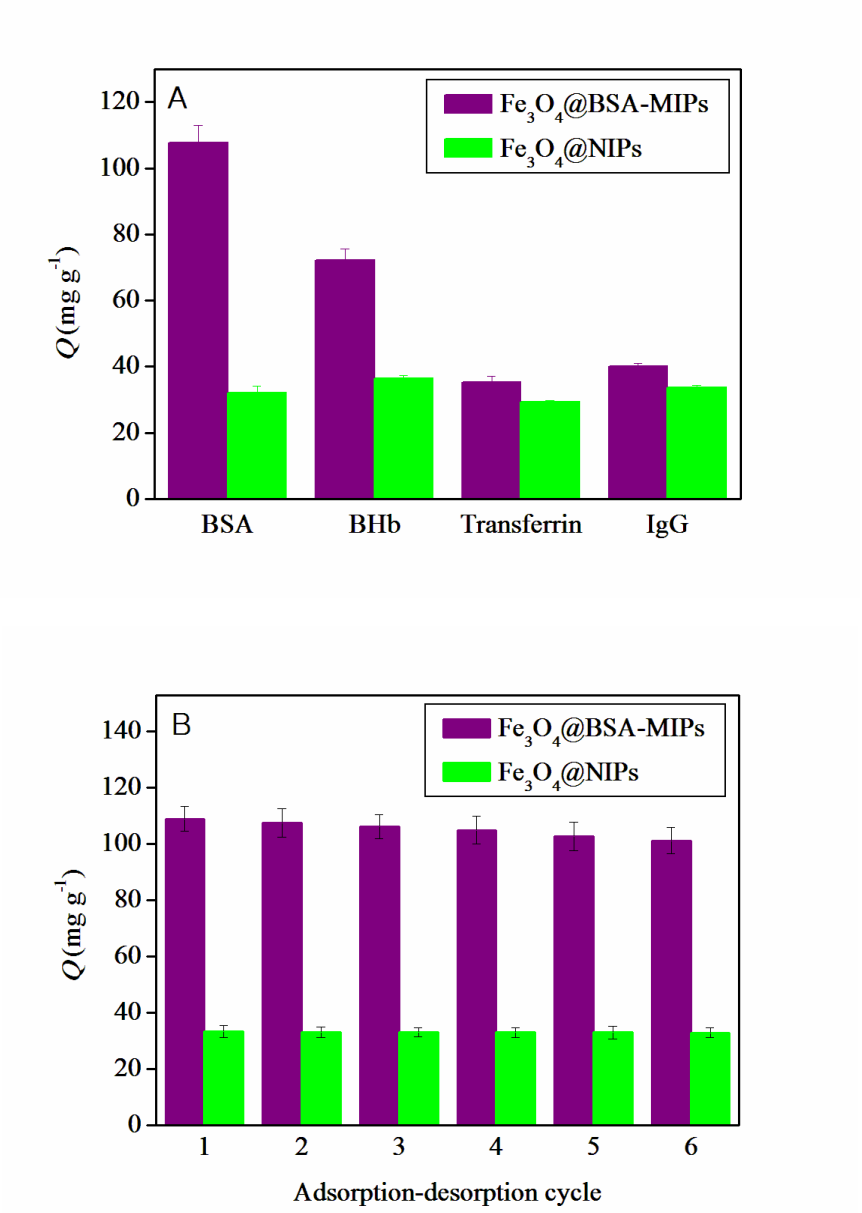

Fig. 8 The specific adsorption capability (A) and reusability (B) of Fe_3O_4@BSA-MIPs and Fe_3O_4@NIPs.

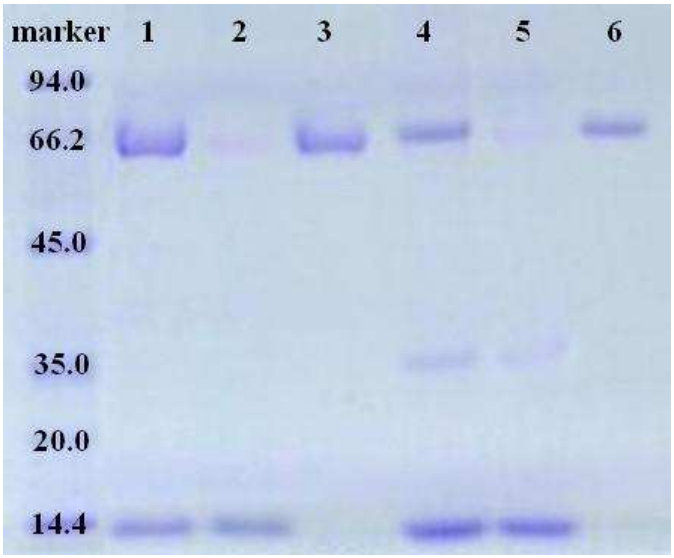

Fig. 9 SDS-PAGE analysis to evaluate the applicability of Fe_3O_4@BSA-MIPs towards BSA. Lane 1, 0.30 mg mL^{-1} BSA and BHb binary standard solution; lane 2, remaining BSA and BHb solution after adsorption by Fe_3O_4@BSA-MIPs; lane 3, the BSA and BHb mixture eluted by 2% SDS-HAc; lane 4, bovine blood diluted 150-fold; lane 5, remaining bovine blood after adsorption by Fe_3O_4@BSA-MIPs; lane 6, the absorbed bovine blood eluted by 2% SDS-HAc.

Table 1

Equations and parameters of adsorption kinetics and isotherms of Fe_3O_4@BSA-MIPs and Fe_3O_4@NIPs.

Model	Equations and Parameters	Fe_3O_4@BSA-MIPs	Fe_3O_4@NIPs
Second-order kinetic	Equation	$t/Q_t = 0.0082 + 0.0091\ t$	$t/Q_t = 0.0989 + 0.0292\ t$
	Q_e (mg g^{-1})	109.9	34.13
	K (g mg^{-1} min^{-1})	0.0101	0.0087
	v_0 (mg g^{-1} min^{-1})	122.0	10.11
	r	0.9998	0.9964
Langmuir isotherm	Equation	$C_e/Q = 2.1162 \times 10^{-4} + 0.0085\ C_e$	$C_e/Q = 0.0019 + 0.0254\ C_e$
	Q_{max} (mg g^{-1})	117.6	39.37
	K_L (mL mg^{-1})	40.18	13.37
	r	0.9969	0.9954
Freundlich isotherm	Equation	$\log Q = 2.2525 + 0.3381\ \log C_e$	$\log Q = 1.7022 + 0.3843\ \log C_e$
	K_F (mg g^{-1})	178.9	50.37
	n	0.3381	0.3843
	r	0.9811	0.9339

Table 2

Comparison of two kinds of imprinted nanoparticles.[a]

Polymers	Q (mg g^{-1})	*IF*
Fe_3O_4@BSA-MIPs	107.8	—
Fe_3O_4@NIPs	32.15	3.35
B-Fe_3O_4@BSA-MIPs	53.19	—
B-Fe_3O_4@NIPs	31.84	1.67

[a] In this experiment, 10 mg of Fe_3O_4@BSA-MIPs, B-Fe_3O_4@BSA-MIPs, Fe_3O_4@NIPs, and B-Fe_3O_4@NIPs were incubated in 10 mL of Tris-HCl (10 mM, pH = 7.0) solution of BSA at a concentration of 0.30 mg mL^{-1} respectively at room temperature for 20 min. (n = 5)

Table 3

Cross-selectivity of BSA, BHb, Hb, RNase A, and Lyz adsorbing by Fe_3O_4@BSA-MIPs, Fe_3O_4@BHb-MIPs, Fe_3O_4@Hb-MIPs, Fe_3O_4@RNase A-MIPs, Fe_3O_4@Lyz-MIPs, and Fe_3O_4@NIPs.[a]

Polymers	Proteins	Q (mg g^{-1})	*IF*	*SC*
Fe_3O_4@BSA-MIPs	BSA	107.8 ± 2.7	3.35 ± 0.02	—
	BHb	72.13 ± 1.8	1.97 ± 0.08	1.70 ± 0.07
	Hb	70.15 ± 1.9	2.05 ± 0.03	1.63 ± 0.04
	RNase A	82.61 ± 2.2	2.01 ± 0.07	1.67 ± 0.11
	Lyz	99.1 ± 3.4	2.10 ± 0.04	1.59 ± 0.09
Fe_3O_4@BHb-MIPs	BSA	73.89 ± 1.7	2.30 ± 0.09	2.16 ± 0.08
	BHb	181.1 ± 3.6	4.96 ± 0.23	—
	Hb	146.3 ± 3.8	4.27 ± 0.26	1.16 ± 0.02
	RNase A	93.82 ± 2.9	2.28 ± 0.07	2.18 ± 0.25
	Lyz	105.7 ± 3.1	2.24 ± 0.05	2.21 ± 0.32
Fe_3O_4@Hb-MIPs	BSA	71.41 ± 2.0	2.22 ± 0.04	2.47 ± 0.16
	BHb	159.2 ± 3.7	4.36 ± 0.06	1.26 ± 0.35
	Hb	187.9 ± 3.5	5.48 ± 0.03	—
	RNase A	91.85 ± 2.4	2.24 ± 0.02	2.45 ± 0.26
	Lyz	109.3 ± 2.9	2.31 ± 0.09	2.37 ± 0.12
Fe_3O_4@RNase A-MIPs	BSA	47.61 ± 2.2	1.48 ± 0.06	4.06 ± 0.12
	BHb	66.22 ± 3.6	1.81 ± 0.03	3.32 ± 0.29
	Hb	63.01 ± 3.9	1.84 ± 0.05	3.27 ± 0.37
	RNase A	246.8 ± 8.3	6.01 ± 0.26	—
	Lyz	136.5 ± 2.7	2.89 ± 0.04	2.08 ± 0.08
Fe_3O_4@Lyz-MIPs	BSA	43.94 ± 1.4	1.37 ± 0.08	4.50 ± 0.13
	BHb	62.73 ± 2.5	1.72 ± 0.03	3.58 ± 0.46
	Hb	59.42 ± 1.9	1.73 ± 0.02	3.56 ± 0.39
	RNase A	119.6 ± 3.6	2.91 ± 0.05	2.12 ± 0.25
	Lyz	291.1 ± 11.2	6.16 ± 0.31	—
Fe_3O_4@NIP	BSA	32.15 ± 0.94	—	—
	BHb	36.54 ± 1.2	—	—
	Hb	34.26 ± 1.4	—	—
	RNase A	41.06 ± 2.9	—	—
	Lyz	47.26 ± 1.3	—	—

[a] In these experiments, 10 mg of Fe_3O_4@BSA-MIPs, Fe_3O_4@BHb-MIPs, Fe_3O_4@Hb-MIPs, Fe_3O_4@RNase A-MIPs, Fe_3O_4@Lyz-MIPs, and Fe_3O_4@NIPs were incubated in 10 mL of Tris-HCl (10 mM, pH = 7.0) solution of BSA, BHb, Hb, RNase A, and Lyz at a concentration of 0.30 mg mL^{-1} respectively at room temperature for 20 min. (n = 5)

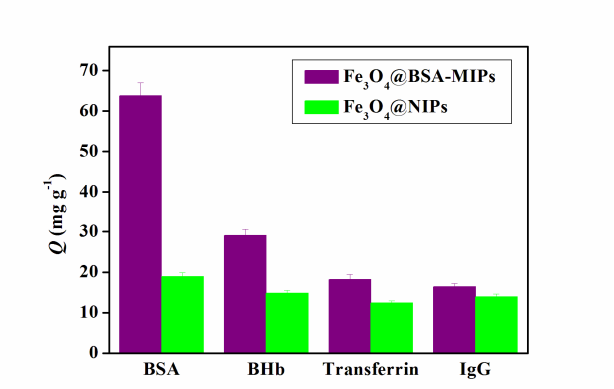

A simple approach for specific depletion of protein using polydopamine imprinting shells modified amino-functionalized magnetic nanoparticles was developed.